Orientation of the Mn(II)−Mn(III) Dimer Which Results from the Reduction of the Oxygen-Evolving Complex of Photosystem II by NO: An Electron Paramagnetic Resonance Study†

Jonathan Hanley,‡ Josephine Sarrou,§ and Vasili Petrouleas*,§

Section de Bioenergetique, URA CNRS 2096, Departement de Biologie Cellulaire et Moleculaire, CEA Saclay, 91191 Gif-sur-Yvette Cedex, France, and Institute of Materials Science, NCSR "Democritos", 15310 Aghia Paraskevi Attikis, Greece

Received April 25, 2000; Revised Manuscript Received July 5, 2000

ABSTRACT: The central part of the oxygen-evolving complex of photosystem II is a cluster of four manganese atoms. The known EPR spectra in the various oxidation states of the cluster are complicated by the magnetic interactions of the four Mn ions and accordingly are difficult to analyze. It has been shown recently that NO at −30 °C slowly reduces the cluster to a Mn(II)−Mn(III) state [Sarrou, J., Ioannidis, N., Deligiannakis, Y., and Petrouleas, V. (1998) *Biochemistry 37,* 3581−3587). We study herein the orientation dependence of the Mn(II)−Mn(III) EPR spectrum with respect to the thylakoid membrane plane. Both the powder and the oriented spectra are satisfactorily simulated with the same set of fine and hyperfine parameters assuming axial symmetry and collinear *g* and *A* tensors. The axial component of the tensors is found to be oriented at an angle of 20° ± 10° to the membrane plane normal (mosaic spread $\Omega = 40°$). We make the reasonable assumption that the Mn(II)−Mn(III) dimer is one of the di-μ-oxo units that has been suggested to comprise the Mn tetramer. On the basis of the sign of the hyperfine tensor anisotropy, the axial direction is assigned to the d_{z^2} orbital of Mn(III), which by comparison with synthetic model complexes is assumed to be oriented perpendicular to the Mn−(μ-oxo)−Mn plane. The present results complement earlier orientation studies by EXAFS and suggest that the Mn−(μ-oxo)−Mn plane makes a small angle (approximately 20°) with the membrane plane and the axis connecting the bridging oxygens is approximately parallel to the plane.

Photosynthetic water cleavage is carried out by the so-called oxygen-evolving complex (OEC)[1] located on the electron donor side of photosystem II (PSII). The OEC stores oxidizing equivalents in four light-driven oxidation steps (S_0-S_1, ..., S_3-S_4) and extracts electrons from water to yield molecular oxygen and protons (see refs *1*−*5* for reviews). The central part of the OEC is a cluster of four manganese atoms. Much of what is known about the structure and the electronic properties of the cluster results from EPR and X-ray absorption fine structure (EXAFS) spectroscopy. It is generally accepted that the cluster contains four manganese atoms, which in the dark stable S_1 state have the following composition: Mn(III, III, IV, IV) (*4*) or $Mn(III)_4$ (*6*). The favored structure of the cluster is a dimer of dimers (*4*) with intra- and interdimer distances of 2.7 and 3.3 Å, respectively, in the S_1 state (*7*−*10*). The former distance is assigned to a di-μ-oxo Mn(III)−Mn(IV) unit while the 3.3 Å distance has been ascribed to a mono-μ-oxo-bis-carboxylato-bridged Mn−Mn unit.

Partially oriented membranes on Mylar sheets have been used in several EPR and EXAFS studies in an effort to obtain orientation information about the cluster axes with respect to the membrane plane. EXAFS experiments indicate that the 2.7 Å vectors are at respective angles of 57° and 68° (*4*, *10*) or, according to more recent estimates, an average angle of 80° (*11*) with respect to the thylakoid normal. Orientation studies of the Mn cluster by EPR spectroscopy have been done mainly on the signals associated with the S_2 state (*12*−*15*) and lately on the S_3 state (*16*). An inherent difficulty in the interpretation of the EPR data is the large set of unknown fine and hyperfine parameters of the cluster. Furthermore, the S_2 state signals show weak orientation dependence.

A new intermediate has been trapped recently by the interaction of NO with the Mn cluster. NO has been shown to act as a sequential one-electron reductant of the Mn cluster. The end product of prolonged incubation of PSII membranes with NO at −30 °C is a Mn(II)−Mn(III) dimer, which is characterized by an EPR signal centered at $g \approx 2$ with prominent hyperfine structure extending over an apparent width of 1600 G (*17*). This signal has been accurately simulated with parameters similar to those of the *Thermus*

†This work was supported by the PENED 1999 program of the Greek General Secretariat of Research and Technology and by EC Grant ERBFMRXCT980214, which supported the stay of J.H. in Greece.

* Corresponding author. Tel: +301 650-3344. Fax: +301 651-9430. E-mail: vpetr@ims.demokritos.gr.

‡ CEA Saclay.

§ Institute of Materials Science.

[1] Abbreviations: PSII, photosystem II; BBY membranes, thylakoid membrane fragments enriched in PSII; S-states, S_0, ..., S_4 oxidation states of the water oxidizing complex; Tyr Y_Z and Tyr Y_D, the fast and slow tyrosine electron donors of PSII; cw EPR, continuous wave electron paramagnetic resonance; MES, 2-(*N*-morpholino)ethanesulfonic acid; chl, chlorophyll; OEC, oxygen-evolving complex; WOC, water oxidizing complex.

10.1021/bi000942g CCC: $19.00
Published on Web 11/17/2000

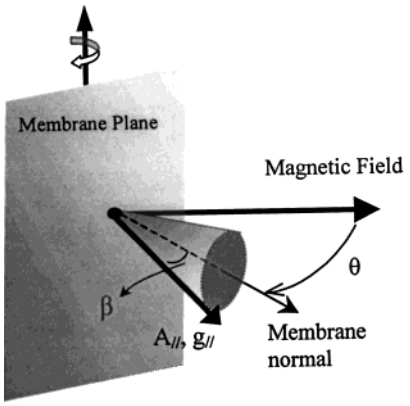

FIGURE 1: Definition of the orientation angles. Angle θ describes the orientation of the applied magnetic field relative to the normal to the thylakoid membrane plane. Angle β describes the orientation of the $A_{||}$ and $g_{||}$ tensor components relative to the membrane normal.

thermophilus catalase (*18*) and appears to result from a state lower than S_0, possibly S_{-2} (*19*). The observation of a magnetically isolated dimer offers a strong tool to the study of the electronic structure of the Mn cluster without the complications added by the interactions with the rest of the cluster.

Here, we present the orientation dependence of the Mn(II)−Mn(III) EPR signal and theoretical simulations. These allow the estimation of the hyperfine and *g* tensor axes orientation, and by extrapolation the molecular axes orientation, with respect to the membrane plane.

MATERIALS AND METHODS

PSII-enriched thylakoid membranes were isolated from market spinach as described previously (*20*). Samples for EPR measurements were resuspended to a concentration of 6−8 mg/mL chl in a buffer containing 0.4 M sucrose, 15 mM NaCl, 5 mM $MgCl_2$, and 40 mM MES, pH 6.5. To orient the samples, this suspension was painted onto strips of Mylar and then dried under a stream of air at 2 °C in the dark for 3−4 h. Ten sheets of prepared Mylar were placed into a 5 mm EPR tube, and the tubes were thoroughly flushed with nitrogen and then sealed. The degree of orientation was verified by measuring the oxidized Y_D signal at a range of angles between 0 and 90° (*12*). The Mn(II)−Mn(III) signal was subsequently generated by the addition of pure NO to the tube under anaerobic conditions at −30 °C followed by incubation of the sample at −15 °C until the signal had developed. Depending on the thickness of the membrane layer, incubation times for the evolution of the maximum Mn(II)−Mn(III) signal ranged from a few days to a month. NO was subsequently removed by evacuation. Spectra of tubes containing unpainted Mylar strips were used to remove background contributions.

The angles of the orientation studies are defined in Figure 1. The membrane plane is parallel to the Mylar sheet. θ is the angle between the external magnetic field and the normal to the membrane plane. The angle β defines the orientation of the axial component of the $g_{||}$ and $A_{||}$ tensors of the Mn dimer relative to the membrane normal. Deviations from perfect alignment are accounted for by the use of the mosaic spread angle Ω (not shown in Figure 1) in the simulations. In these one dimensionally oriented samples, orientations of the magnetic field at angles θ, $\pi - \theta$, $\pi + \theta$, and $2\pi - \theta$ are equivalent. Accordingly, experiments in the first quadrant would suffice to determine the principal axes orientation. To reduce errors due to misalignment of the Mylar sheets and changes in the filling factor of the EPR cavity, a full set of spectra over 360° for every 10° was obtained. Polar plots of spectral features showing a strong orientation dependence were used to correct the 0° of the "θ" scale with an accuracy of ±5°. The data were reduced to the first quadrant by the addition of the spectra at symmetric angles (see above).

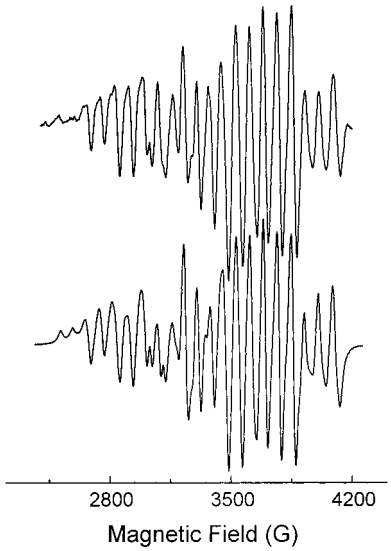

FIGURE 2: (Upper trace) Powder spectrum resulting from the averaging of four individual spectra (see text). (Lower trace) Least-squares fitting assuming collinear *g* and *A* tensors and the following values of the parameters: for Mn(II), $A_{||} = -762$ MHz, $A_{\perp} = -549$ MHz; for Mn(III), $A_{||} = 200$ MHz, $A_{\perp} = 222$ MHz; $g_{||} = 2.011$, $g_{\perp} = 1.970$. EPR conditions: $T = 11$ K; microwave frequency, 9.42 GHz; microwave power, 31 mW; modulation amplitude, 25 Gpp.

X-band EPR spectra were obtained with a Bruker ER-200D-SRC spectrometer interfaced to a personal computer and equipped with an Oxford ESR 900 (above 4 K), an Anritsu MF76A frequency counter, and a Bruker 035M NMR gauss meter.

The simulation program of the powder spectrum was modified for the simulation of the oriented membrane spectra, based on the procedure described by Blum et al. (*21*). As was pointed to us by the reviewers [and previously noted by Schiller et al. (*11*), the approach of Blum et al. (*21*) is not fully correct in the treatment of the mosaic spread. We accordingly modified our simulation program to correct for this (*11*). This resulted in a small shift (3 deg) of the final angle β and a somewhat improved fit to the experimental spectra.

RESULTS

Nonoriented (Powder) Spectrum. The simulation of the nonoriented spectrum has been reported earlier (*18*). An improved experimental spectrum—the average of four individual spectra following subtraction of the background spectra obtained by a 10 min incubation at −5 °C (*18*)—is shown in Figure 2 (upper trace). A least-squares fit of the spectrum in Figure 2 (lower trace) gave values for the *g* and hyperfine tensors (see figure caption) practically identical to the published set (*18*). These values of the *g* and *A* tensors were used as constants in the simulation of the oriented spectra.

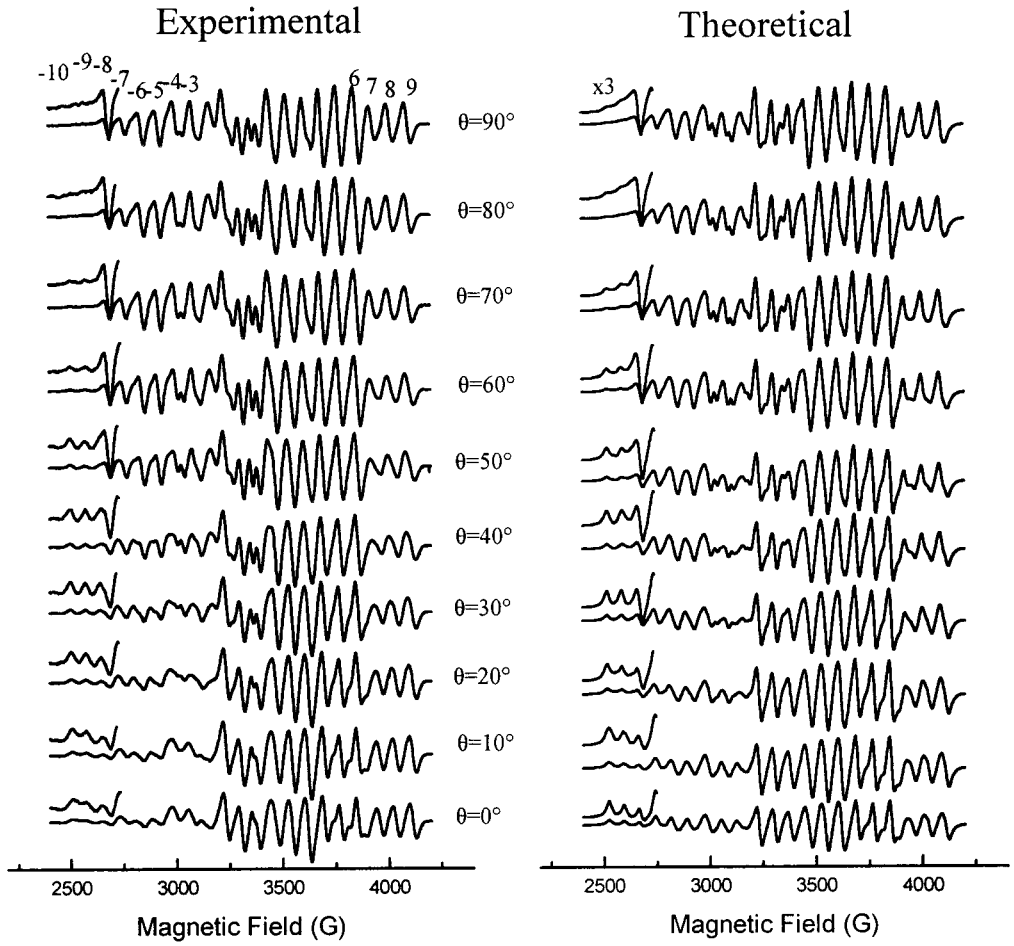

FIGURE 3: Experimental spectra of oriented PSII membrane samples reduced to the first quadrant as described in Materials and Methods and theoretical simulations with $\beta = 20°$ and $\Omega = 40°$. Angles are as defined in Figure 1. EPR conditions are as in Figure 2.

Spectra of Oriented Membranes. Oriented spectra reduced to the first quadrant (see Materials and Methods) are shown in Figure 3. Examination of the spectra shows that there is a significant orientation dependence of the Mn(II)−Mn(III) multiline signal. This is in contrast to the weak orientation of the S_2 multiline signal (*12*, *13*). When the magnetic field is parallel to the membrane, $\theta = 90°$, the spectrum looks similar to the powder spectrum. Significant deviations are observed as the field moves out of the membrane plane and toward the vertical to the membrane. The intensity of the outer +7, +8, and +9 peaks varies and a slight shift in their position occurs, while a progressive splitting and decrease in the intensity of the +5 and +6 peaks is observed with decreasing θ angle below 30°. The left-hand side of the spectra shows more pronounced changes. The intensity of most peaks decreases significantly as the magnetic field angle θ decreases below 60°. Notable is the variation of the weak outer peaks in the low-field part of the spectra. These increase progressively with decreasing angle θ and appear to have a maximum at about $\theta = 30°-10°$. It is shown below that this coincides with the orientation of an anisotropy axis.

The spectral window in Figures 2 and 3 was reduced to a minimum—not excluding any Mn contributions—in order to reduce computing time. Spectra over a broader magnetic field range at two angles, 0° and 90°, are included as Supporting Information. These contain, in addition, the $g_z \approx 3$ component of the high-potential cyt b_{559}. This species is spontaneously oxidized during the early stages of the NO treatment (Ch. Goussias and V. Petrouleas, paper in preparation). The $g_y \approx 2.2$ component of cyt b_{559} at about 3000 G, which is maximum at 0° relative to the membrane normal (see ref *12* and references cited therein), interferes with the Mn(II)−Mn(III) signal at the position of the −3 and −4 peaks in Figure 3. The orientation dependence of the $g_z \approx 3$ component of the cyt b_{559}, included as Supporting Information, was utilized to obtain initial estimates of the mosaic spread parameter, Ω.

Theoretical Simulations of the Oriented Spectra. Simulation of the oriented spectra for several angles θ of the magnetic field relative to the membrane normal was done assuming the same symmetry (axial symmetry and collinear axes) and the same values of the tensors as in the powder spectrum (*18*). Because of the axial symmetry of the tensors the only angular parameter that needs to be defined is the angle of the axial component of the tensors relative to the membrane normal: angle β in Figure 1.

Simulations of the spectra were done for a broad range of angle β values. Only β angles in the range 10°−30° gave acceptable simulations of all spectra. For larger angles β the variation of the simulated spectra as a function of the angle θ showed gross incosistencies with the experimental spectra. The simulation was refined by varying the mosaic spread between 30° and 50°. This was followed by a fitting procedure which yielded $\beta = 20° \pm 10°$ and $\Omega = 40°$. The theoretical spectra calculated with these values of the parameters are shown in Figure 3. The agreement with the

experimental spectra appears to be satisfactory extending to the details. The deviation in the vicinity of peaks −3 and −4 is due, as we noted already, to the contribution of the g_y component of cyt b_{559} to the experimental spectra. The fitting could be improved possibly further if the restriction of axial symmetry and collinearity of the *g* and *A* tensors was relaxed, but this would introduce too many unknown parameters.

Consequently, the $g_{||}$ and $A_{||}$ tensor components of the dimer make an angle of 20° ± 10° with the membrane plane.

DISCUSSION

The present results indicate a significant orientation dependence of the Mn(II)−Mn(III) EPR spectrum. The spectra at different orientation angles have been successfully simulated with the same set of hyperfine and *g*-tensor parameters—assuming axial symmetry and collinear *g* and *A* tensors—that was used to fit the powder spectrum. The axial direction, defined by the parallel component of the *A* and *g* tensors, is found to be oriented at an angle of approximately 20° relative to the normal to the membrane plane.

In Mn(II)−Mn(III) dimers the Mn(III) ion is expected to be the main source of anisotropy (*22*, *23*). Assuming $S = 2$ and a tetragonally distorted octahedral ligand field environment, the ground electronic configuration of this ion will be either $d_{xy}^1\ d_{yz}^1\ d_{zx}^1\ d^1{}_{z^2}$ or $d_{xy}^1\ d_{yz}^1\ d_{zx}^1\ d^1{}_{x^2-y^2}$. The sign of $\Delta\alpha = \alpha_z - \alpha_x$ is positive for the former and negative for the latter configuration (*23*, *24*). In the present case $\Delta\alpha$ is positive (*18*), and therefore the fourth electron occupies the d_{z^2} orbital. Accordingly, the d_{z^2} orbital must define the axial direction in the complex. The determination of the orientation of the d_{z^2} orbital with respect to the molecular axes is less straightforward. The data on Mn(II)−Mn(III) dimers are scarce. Insights can be obtained by examination of Mn(III)−Mn(IV) complexes, where the anisotropy is also determined by the Mn(III) ion. In synthetic Mn(III)−Mn(IV) complexes with μ-oxo bridges Gamelin et al. (*25*) show that the *x*-axis is along the line connecting the two Mn ions, the *y*-axis is parallel to the line connecting the two μ-oxygen atoms, and the *z*-axis is perpendicular to the plane defined by Mn(III), the oxygen bridges, and Mn(IV) (see also ref *22*). It is reasonable to assume a similar molecular axes arrangement in the present case placing the axial direction of the Mn(II)−Mn(III) dimer orthogonal to the plane of the bridge and the Mn ions. Accordingly, the plane of the bridge must be oriented approximately at an angle of 20° with respect to the membrane plane.

It would be instructive to compare the Mn(II)−Mn(III) orientation results with the orientation studies by EXAFS. As the latter have been discussed in the context of the dimer of dimers model (*4*), we will limit the discussion to this structural arrangement allthough clearly the present results are not restricted to this particular model. According to the dimer of dimers model (*4*), two di-μ-oxo-bridged Mn dimers are connected by a mono-μ-oxo bridge and two bis-carboxylato bridges. The Mn−Mn distance in the S_1 state in each of the di-μ-oxo-bridged dimers is 2.7 Å, and that between the Mn atoms linked by the mono-μ-oxo bridge is 3.3 Å. The vector formed by the 3.3 Å manganese pair is oriented almost perpendicular to the membrane plane, while the 2.7 Å vectors are oriented with average angles of 60 ± 7° (*4*, *10*) or, according to more recent estimates, 80° (*11*) with respect to the membrane normal. In the context of the "dimer of dimers" model it is reasonable to assume that the magnetically isolated Mn(II)−Mn(III) pair is one of the two "2.7 Å" dimers. It will be difficult otherwise to explain the absence of magnetic coupling with the rest of the cluster. This assignment would also lead to a consistent picture in combination with the EXAFS data, as discussed below. The Mn−Mn distance may appear small compared to what is extrapolated for the Mn(II)−Mn(III) state of the *T. thermophilus* catalase on the basis of a 2.87 Å distance in the Mn(III−IV) state (*27*), a 3.13 Å distance in the (III−III) state (*28*), and a distance which varies between 3.18 Å (no additions) (*27*), 3.3 Å (addition of chloride) (*28*), or 3.5 Å (addition of phosphate) in the (II, II) state (V. Barynin, personal communication). It has been suggested, however, by EXAFS studies of the PSII complex that one of the 2.7 Å distances increases to 2.85 Å upon reduction of the S_1 to the S_0 state. It is likely that the Mn−Mn distance in Mn(II)−Mn(III), which is a lower oxidation state than S_0 (*19*), increases further due to the protonation of both oxygen bridges. This could make the distance comparable to what is expected for Mn catalase. The 3.3 Å distance could similarly increase and result in an elimination of the interdimer magnetic coupling. Significantly more drastic assumptions are to be made if the Mn(II)−Mn(III) dimer is assigned to the "3.3 Å" couple. The 3.3 Å distance must remain unchanged or even decrease somewhat, while the two intradimer 2.7 Å distances must increase far in excess (all bridges practically removed) to eliminate the magnetic couplings.

The present data offer complementary information to the orientation studies by EXAFS. The latter show that the Mn−Mn axis—*x*-axis in the present notation—makes a large angle, 60° (*4*, *10*), or according to more recent estimates 80° (*11*), with the membrane normal. The present data show that the axis vertical to the Mn−(μ-oxo)-Mn plane—*z* axis—makes a small angle, 20°, with the membrane normal. As the two angles are approximately complementary, the membrane normal must approximately lie on the *xz* plane (otherwise, the sum of the two angles would be much higher than 90°). Therefore, the *xz* plane is approximately perpendicular to the membrane plane, and consequently the *y*-axis—axis connecting the two oxygens—is parallel to the membrane plane. This arrangement, which was favored by earlier EXAFS studies (*11*), is shown in Figure 4.

The proposed arrangement in Figure 4 is at variance with the geometric model suggested in an earlier study of the S_2 multiline signal (*13*). Hasegawa et al. proposed that the vector connecting the two μ-O nuclei of one of the dimers [assumed to be a Mn(III)−Mn(IV) couple] makes an angle of 43°−56° with the thylakoid membrane normal (i.e., 34°−47° with respect to the membrane plane) (*13*). To explain the difference, one might assume that the two studies detect different dimers. It should be noted, however, that the analysis of the S_2 multiline inevitably relies on a large number of unknown parameters, and furthermore, the extraction of orientation information is complicated by the weak orientation dependence of this signal.

In conclusion, the present results show a significant orientation anisotropy of the magnetic axes of the Mn(II)−Mn(III) dimer. Assuming μ-oxo bridges between the two Mn

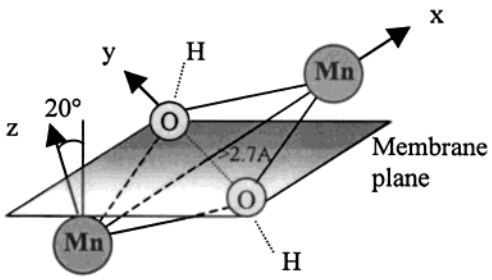

FIGURE 4: Proposed orientation of the Mn(II)−Mn(III) dimer with respect to the membrane plane based on the results of the present simulation study and previously reported EXAFS studies (see text for details).

ions, the analysis of the data suggests that the Mn−(μ-oxo)−Mn plane makes a small angle (20° ± 10°) with the membrane plane. Combination of this result with earlier orientation studies by EXAFS suggests that the axis connecting the bridging oxygens is approximately parallel to the plane. Nothing can be said from the present data on the arrangement of the rest of the Mn cluster.

ACKNOWLEDGMENT

We thank Dr. N. Ioannidis, Dr. Ch. Goussias, and Dr. Y. Deligiannakis for helpful advice and discussions.

SUPPORTING INFORMATION AVAILABLE

Two figures showing representative oriented spectra of the Mn(II)−Mn(III) signal and the cyt b_{559} at 0° and 90° with respect to the membrane normal and the orientation dependence of the oxidized high-potential cyt b_{559} signal at $g \cong 3$. This material is available free of charge via the Internet at http://pubs.acs.org.

REFERENCES

1. Rutherford, A. W. (1989) *Trends Biol. Sci. 14*, 227−232.
2. Hansson, O., and Wydrzynski, T. (1990) *Photosynth. Res. 23*, 131.
3. Debus, R. J. (1992) *Biochim. Biophys. Acta 1102*, 269−352.
4. Yachandra, V. K., Sauer, K., and Klein, M. P. (1996) *Chem. Rev. 96*, 2927−2950.
5. Britt, R. D. (1996) *Advances in Photosythesis*: *Vol. 4. Oxygenic Photosynthesis: The Light Reaction* (Ort, R. D., and Yocum, C. F., Eds.) pp 137−164, Kluwer Academic Publishers, Dordrecht.
6. Zheng, M., and Dismukes, G. C. (1996) *Inorg. Chem. 35*, 3307−3319.
7. Yachandra, V. K., DeRose, V. J., Latimer, M. J., Mukerji, I., Sauer, K., and Klein, P. (1993) *Science 260*, 675−679.
8. George, G. N., Prince, R. C., and Cramer, S. P. (1989) *Science 242*, 789−791.
9. Penner-Hahn, J. E., Fronko, R. M., Pecoraro, V. L., Yocum, C. F., Betts, S. D., and Bowlby, N. R. (1990) *J. Am. Chem. Soc. 112*, 2549−2557.
10. Mukerji, I., Andrews, J. C., DeRose, V. J., Latimer, M. J., Yachandra, V. K., Sauer, K., and Klein, M. P. (1994) *Biochemistry 33*, 9712−9721.
11. Schiller, H., Dittmer, J., Iuzzolino, L., Dorner, W., Meyer-Klaucke, W., Sole, V. A., Nolting, H. F., and Dau, H. (1998) *Biochemistry 37*, 7340−7350.
12. Rutherford, A. W. (1985) *Biochim. Biophys. Acta 807*, 189−201.
13. Hasegawa, K., Kusunoki, M., Inoue, Y., and Ono, T. (1998) *Biochemistry 37*, *26*, 9457−9465.
14. Smith, P. J., Ahrling, A. K., and Pace, R. J. (1993) *J. Chem. Soc., Farad. Trans. 89*, 2863−2868.
15. Kim, D. H., Britt, R. D., Klein, M. P., and Sauer, K. (1992) *Biochemistry 31*, 541−547.
16. Matsukawa, T. Mino, H., Yoneda, D., and Kawamori, A. (1999) *Biochemistry 38*, 4072−4077.
17. Goussias, Ch., Ioannidis, N., and Petrouleas, V. (1997) *Biochemistry 36*, 9261−9266.
18. Sarrou, J., Ioannidis, N., Deligiannakis, Y., and Petrouleas, V. (1998) *Biochemistry 37*, 3581−3587.
19. Ioannidis, N., Sarrou, J., Schansker, G., and Petrouleas, V. (1998) *Biochemistry 37*, 16445−16451.
20. Berthold, D. A., Babcock, G. T., and Yocum, C. F. (1981) *FEBS Lett. 134*, 231−234.
21. Blum, H., Salerno, J. C., and Leigh, J. S., Jr. (1978) *J. Magn. Reson. 38*, 385−391.
22. Shafer, K., Bittl, R., Zweygart, W., Lendzian, F., Haselhorst, G., Weyhermuller, T., Weighardt, K., and Lubitz, W. (1998) *J. Am. Chem. Soc. 120*, 13104−13120.
23. Zheng, M., Khangulov, S. V., Dismukes, G. C., and Barynin, V. V. (1994) *Inorg. Chem. 33*, 382−387.
24. Gerritsen, H. J., and Sabinsky, E. S. (1963) *Phys. Rev. 132*, 1507−1512.
25. Gamelin, D. R., Kirk, M. L., Stemmler, T. L., Pal, S., Armstrong, W. H., Penner-Hahn, J. E., and Solomon, E. I. (1994) *J. Am. Chem. Soc. 116*, 2392.
26. Messinger, J., Robblee, H. J., Fernandez, C., Cinco, R. M., Visser, H., Bergmann, U., Glatzel, P., Cramer, S. P., Campbell, K. A., Peloquin, J. M., Britt, R. D., Sauer, K., Yachandra, V. K., and Klein, P. M. (1998) *Photosynthesis: Mechanisms and Effects* (Garab, G., Ed.) Vol. II, pp 1279−1282, Kluwer Academic Publishers, Dordrecht/Boston/London.
27. Barynin, V. V., Hempstead, P. D., Vagin, A. A., Antonyuk, S. V., Melik-Adamyan, V. R., Lamzin, V. S., Harrison, P. M., and Artymiuk, P. J. (1998) EMBL Hamburg Outstation Annual Report, EMBL Hamburg Outstation at Deutsches Elektronen-Synchrotron DESY, D-22603 Hamburg, Germany.
28. Antonyuk, S. V., Melik-Adamyan, V. R., Popov, A. N., Lamzin, V. S., Hempstead, P. D., Harrison, P. M., Artymiuk, P. J., and Barynin, V. V. (2000) *Crystallogr. Rep. 45*, 105−116.

BI000942G